

Use of surface-enhanced Raman spectroscopy for the detection of human integrins

Mustafa H. Chowdhury

V. Alexander Gant

Texas A&M University
Department of Biomedical Engineering
College Station, Texas 77843-3120

Andreea Trache

Texas A&M University
Department of Medical Physiology
College Station, Texas 77843-1114

Angela Baldwin

Texas A&M University
Department of Biomedical Engineering
College Station, Texas 77843-3120

Gerald A. Meininger

Texas A&M University
Department of Medical Physiology
College Station, Texas 77843-1114

Gerard L. Coté

Texas A&M University
Department of Biomedical Engineering
College Station, Texas 77843-3120
E-mail: gcote@tamu.edu

1 Introduction

The ability of live cells to adhere to one another and to the extracellular matrix (ECM) is essential to their survival and functionality. This “stickiness” of cells drives many processes in the body such as embryonic development, blood clotting, wound healing, and eradication of infection.¹ Unfortunately, this property of the cells also contributes to a number of disorders of the body, such as rheumatoid arthritis, heart attack, stroke, and cancer. The last 15 years of research have shed light on a group of cell-surface molecules called integrins that play a central role in many cell-adhesion-related phenomena.¹ Integrins are a family of cell-surface proteins that are responsible for a wide variety of biological activities such as the adhesion and connection of adjacent cells, blood clotting, vascular remodeling, wound healing, gene expression, etc.¹⁻⁷ Integrins are transmembrane heterodimer protein receptors that adhere to both the intracellular matrix and the ECM and generally consist of two protein subunits. The α subunit is known today to have 15 variants and the β subunit has eight variants. These subunits then combine to form 24 different known integrins.¹⁻⁴ Integrins can play a critical role in the process of thrombosis and cell development, can act as signaling trans-

Abstract. Current research has revealed the importance of a class of cell surface proteins called integrins in various vital physiological functions such as blood clotting, regulation of blood pressure, tissue blood flow, and vascular remodeling. The key to integrin functionality is its ability to mediate force transmission by interacting with the extracellular matrix and cytoskeleton. In addition, they play a role in signal transduction via their connection with the proteins in focal adhesion (FA) points. To understand the complex mechanism of cell-cell and cell-extracellular matrix (ECM) adhesion that is responsible for these diverse biochemical interactions, it is necessary to identify the integrins on cells and monitor their interaction with various ligands. To this end, for the first time, we employ surface-enhanced Raman spectroscopy (SERS) to detect integrins. The results show the capability using SERS to detect the integrins to the nanomolar concentration regime and to distinguish between two different kinds of integrins, $\alpha V\beta 3$ and $\alpha 5\beta 1$, that are present in vascular smooth muscle cells (VSMCs). It is anticipated that the SERS approach will potentially help elucidate the mechanism of integrin-ligand interactions in a variety of phenomena of physiological importance. © 2006 Society of Photo-Optical Instrumentation Engineers. [DOI: 10.1117/1.2187022]

Keywords: surface-enhanced Raman spectroscopy; Raman spectroscopy; integrin; vascular smooth muscle cells.

Paper 05113R received May 3, 2005; revised manuscript received Oct. 31, 2005; accepted for publication Dec. 1, 2005; published online Mar. 22, 2006.

duction pathways passing signals from the ECM to the intracellular matrix and vice versa, and can also play a role as receptors for viruses and bacteria.^{1,2,4} Because of their large involvement in cell processes, there is growing interest in further investigating their behavior. Some examples of the integrin receptors binding to their target molecule are described in the next few sentences. The integrin $\alpha II\beta 3$ displayed on blood platelets binds with fibronectin in the ECM that induce blood clots and vessel occlusion.¹ The integrin $\alpha V\beta 3$ displayed in endothelial cells and smooth muscle cells binds with fibronectin in angiogenesis, thereby contributing to tumor progression and diabetic retinopathy.¹ The integrin $\alpha 4\beta 1$ displayed on various white blood cells binds to fibronectin to cause asthma and arthritis.¹ Many of these diseases are adhesion-related diseases due to integrins that are overactive. In some cases, even bacteria and microbes that cause and aggravate infections can enter healthy cells by attachment to the integrins, since the integrins act as receptors to many molecules.¹ A good example of how integrins could help spread disease in a patient is in cancer propagation. It has long been known that one of the main causes in the spread of cancerous tissues throughout a patient's body is by angiogenesis (growth of new blood vessels). When new blood vessels are formed, endothelial cells as well as smooth muscle cells

Address all correspondence to Gerard Coté, Dept. of Biomedical Engineering, Texas A&M University, Mail Stop 3120, College Station, TX 77843-3120. Tel: 979-845-4196. Fax: 979-845-4450. E-mail: gcote@tamu.edu

are the cells most involved with vessel formation. The integrin $\alpha V\beta 3$ appears in endothelial cells and the smooth muscle cells (SMCs) as the new blood vessels are forming. This integrin plays the major role in adhesion of an endothelial cell (EC) or SMC to its adjacent cell. Thus, if drugs are blocking the $\alpha V\beta 3$ adhesion, then the angiogenesis could be stopped, preventing cancer growth and proliferation. This could be a milestone in the fight against cancer.¹ To understand this complex mechanism of cell-cell and cell-ECM adhesion that is responsible for the diverse biochemical interactions hitherto mentioned, it is necessary to first identify the receptors on cells that act as the “docking” sites for matrix proteins and other cells.

Traditional dispersive Raman spectroscopy is an inefficient tool for the detection of bioanalytes. This is due to the relatively low number of Raman scattered photons compared to Rayleigh scattered ones.⁸ Also, in most biological applications, broadband fluorescence signals of much higher intensity than Raman signals are generated by various molecules in an assay, which create major challenges for obtaining meaningful quantitative Raman signals.⁸ These factors demand the use of highly sophisticated equipment to use Raman spectroscopy for analyte detection at trace levels.

Surface-enhanced Raman spectroscopy (SERS) is a technique developed more recently, which has been used quite successfully to enhance the Raman cross section of a molecule by factors of 10^6 or more.^{9–14} This is done by using low- to medium-powered lasers to excite vibrational transitions in molecules adsorbed on a rough metallic surface. The metallic surface can be in the form of a thin layer of the metallic film on an electrode or glass slide, or in the form of aqueous colloidal nanoparticles. Typical metals used for SERS are gold, silver, and copper. The exact nature of the enhancement of Raman signals through SERS is not fully understood, but it appears to be caused by two contributing mechanisms of enhancement, namely, the electromagnetic mechanism and the chemical mechanism.

The electromagnetic mechanism explains this enhancement primarily due to localized surface plasmon resonance, which is the excitation of the collective oscillation of the conduction band electrons localized on a metal particle by the incident electromagnetic radiation.⁹ The surface plasmon resonance effect creates a radiating dipole in the metal particle and this causes a high-energy field at the particle surface that rapidly decays away from it. Therefore, the incident electromagnetic field acting on an analyte molecule adsorbed onto the surface of the metal particle is increased through the addition of this high-energy field from the metal particle.⁹ Thus, the analyte in close proximity to the metal nanoparticle will experience an increase in field intensity when compared to a molecule in free space (or not in proximity to the metal surface). This increase in the field intensity experienced by the analyte will lead to an increase in its Raman scattered signal.^{10,11} If the Raman-shifted radiation from the analyte molecule is still at a frequency within the width of the plasmon resonance band of the metal surface, the enhancement of the outgoing Raman radiation from the molecule at the metal surface will be increased by an additional multiplicative factor. Thus, the metal surface acts as an amplification “antenna,” which both amplifies the incident field that the analyte molecule experiences as well as the Raman scattered light radiat-

ing off the analyte molecule.¹⁰ It can clearly be deduced that the SERS signal is particularly strong when the laser excitation as well as the Raman scattered radiation are in resonance with the surface plasmon resonance band of the metal. This is generally the case for low-frequency Raman modes of an analyte and helps explain the fact that the intensity of different Raman bands in a SERS spectrum falls off with increasing vibrational energy.^{10,11}

Most SERS-active systems in reality, however, consist of assemblies of interacting metal nanoparticles such as aggregated colloidal metal nanoparticles, rough metal surfaces, and metal island films. Recent theoretical studies and reviews have reported that when two nanoparticles are brought close together (<1 nm), the optical field strength in the space between the particles is greatly enhanced and electromagnetic SERS enhancements of a Raman analyte trapped in this space can reach 10^{11} , providing incident light of the appropriate wavelength is used.^{15–18} This huge enhancement far exceeds the case of an isolated metal nanoparticle (by several orders of magnitude) and occurs because the dipole induced in each nanoparticle arises from the combined effect of the incident light along with the influence of the intense field of the second particle leading to an amplification of the polarization of the dipole in each nanoparticle.^{15–18} This enhancement reaches a maximum when the polarization of the incident light is along the interparticle axis. It has also been reported that particles with sharp protrusions (such as nanorods) create large electromagnetic enhancement at the sharp edges due to increased confinement of surface charge density.¹⁵

It is believed^{15,17–26} that such “hot sites” with very large spatially confined electromagnetic field strengths are primarily responsible for the observation of “single-molecule” SERS (SM-SERS). This phenomena was first reported independently by Kneipp et al.¹⁹ and Nie and Emory²⁰ and has since played a crucial role in elucidating the fundamental mechanism behind SERS. SM-SERS studies have confirmed that extremely large enhancement factors of the order of 10^{14} to 10^{15} can be obtained at such optically “hot” nanostructures. Another interesting feature of SM-SERS is the observation of the SERS signal in an intermittent on and off fashion when observed on a millisecond to second timescale, a phenomenon called “blinking,” which is not present in ensemble averaged SERS studies.^{15,17–26} It has also been reported in recent studies that chloride and other halide ions increase the SERS efficiency (in both SM-SERS and ensemble SERS) by up to two to three orders of magnitude.^{21,26} The “blinking” effect and the high enhancement factors in SM-SERS, the rarity of the “hot sites” in metallic nanostructures, and the effect of halide anion activation indicates the existence of additional chemical enhancement mechanisms and the role of surface active sites in the SERS phenomenon. These chemical enhancement methods include direct charge transfer between the Raman active molecule and the metallic nanostructure; strong electronic coupling between the adsorbed molecule and the metallic active site, which generates new metal-ligand or ligand-metal charge transfer states that can be broadly excited by visible light; resonance Raman effects, which occur due to shifted and broadened electronic levels in the adsorbate molecule as a result of the influence of the metal; and induced modeling of the surface tunneling barrier for electrons and excitation of electron-hole pairs requiring atomic scale rough-

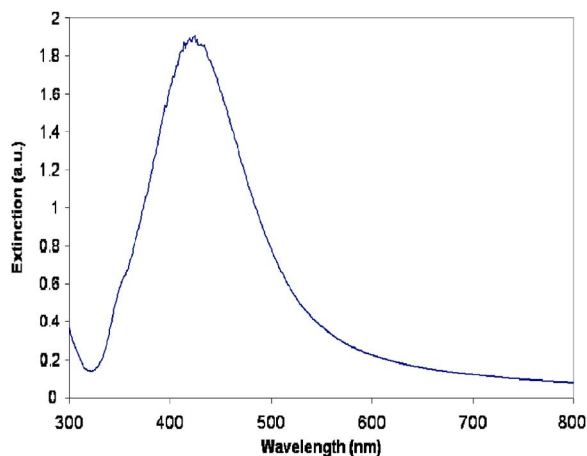


Fig. 1 Extinction spectra of citrate-reduced Ag colloids used for SERS study.

ness among others.^{9,10,12,14,18–24} The role of halide anion activation can be explained by an increased charge transfer (CT) contribution to the total enhancement, increase in electromagnetic enhancement caused by aggregation of colloidal particles (for metal sols only), anion-induced favorable reorientation of the adsorbed molecule relative to the metallic surface or increased adsorption of Raman molecule on metal surface due to effects of coadsorption of halide anions.²⁶ The “blinking” phenomena in SM-SERS is thought to be caused either by photoinduced ionization of the adsorbed molecule, reversible activation and quenching of the chemical enhancement at an active site, or the slow diffusion of the adsorbed molecule between optically active and inactive site on the metallic surface.^{20–26}

SERS has been widely used in biomedical applications for over 2 decades. Early biomedical applications of SERS involved the use of aqueous colloidal silver nanoparticles to study a variety of aromatic and aliphatic amino acids to determine the specific Raman bands associated with these molecules in physiologically relevant conditions.^{27–29} Other SERS studies reported the use of aqueous colloidal gold nanoparticles to study the effects of pH on the conformation of monomeric amino acids and their polymers as well as the nature of their adsorption to colloidal surfaces.^{30,31} Aqueous metal colloidal nanoparticles have also been used extensively to study the SERS spectra of various proteins as well the nature of interaction of drugs with different proteins such as the interaction of the antiretroviral drug hypericin with serum albumins.^{32–36} Such biomedical application for SERS can be of crucial importance in the development of new drugs for curing a variety of fatal diseases.^{35,36} Colloidal metal nanoparticles have also been extensively used for the characterization and detection of individual nucleosides, oligonucleotides, and nucleic acids at physiologically relevant concentrations.^{37–41} Others have used metal colloidal nanoparticles as SERS platforms to study the differences in structure and nature of adsorption of intrinsically “straight,” “bent,” and “kinked” oligonucleotides.⁴² Kneipp et al.⁴³ reported the first use of colloidal gold nanoparticles for the detection of biological molecules such as various nucleic acids and proteins inside cells grown in cell culture. Others have made use

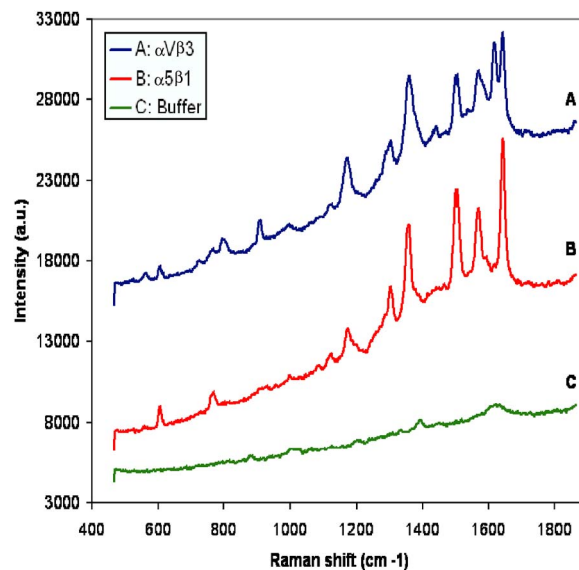


Fig. 2 Raw, unprocessed, SERS spectra of 133-nM $\alpha 5\beta 1$ integrin, 122-nM $\alpha V\beta 3$ integrin, and buffer only (background spectra).

of novel aggregated-gold-nanoparticle-coated SiO_2 chips to detect various strains of gram-positive and gram-negative bacteria.⁴⁴

SERS has also been used for the creation of microarray type gene probes for the detection of cancer^{45–47} as well as in a variety of ELISA (enzyme-linked immunosorbent assay)-like techniques for the detection of mouse immunoglobulin G (IgG; Ref. 48) and the enzymes prostaglandin H synthetase-1 and -2 in normal human hepatocytes and human hepatocellular carcinoma (HepG2) cells.⁴⁹ These techniques adapt a regular ELISA-type assay by replacing the chromogenic readout of the enzyme reaction with nanoparticle-based SERS detection. Another group of studies reported the application of a novel class of SERS active nanostructures for biodetection.^{50–52} These studies use an initial gold nanoparticle bound to both a Raman reporter molecule (giving signal specificity) and a protein (which acted as the biorecognition element). After binding of this conjugate with the target analyte, electroless deposition techniques were employed to develop a silver shell around the gold seed in a process termed “silver enhancement.” The gold seed is used as it generally binds well many biological molecules via oxidation of the surface thiol groups; thus giving the necessary specificity for the secondary silver layer. This silver layer possessed the required size and nanoscale surface roughness to provide efficient SERS enhancement from the reporter molecule. This seeded growth method has been used for nucleic acid detection as well as being extended to protein detection in cells and tissue.^{50–52} An innovative application of SERS was reported by Mulvaney et al.,⁵³ who used nanoparticles bound to a Raman reporter molecule such as rhodamine 6G and encapsulated by silica in multiplexed bioassays. The encapsulated particles were stable in the presence of high salt content (common in biological buffers), because the silica protected the nanoparticles from the environment as well as protecting the environment from the potentially toxic reporter molecule. Recent studies have also shown the use of silver films on nanospheres (AgFON) as SERS substrates for the detection of the anthrax

spore *Bacillus subtilis* with a limit of detection (LOD) of approximately 2.6×10^3 spores. This is well below the anthrax infectious dose of 10^4 spores, and hence the study represents an important step in the eventual development of a portable sensing system for the real-time detection of biowarfare agents for field applications.^{54,55} Haynes et al.,⁵⁵ Shafer-Peltier et al.,⁵⁶ and Stuart et al.⁵⁷ also developed a novel SERS sensing mechanism for the detection of glucose in physiological concentrations using a biocompatible self-assembled partition layer to overcome the poor affinity of glucose to silver surfaces. These findings can represent a milestone toward the development of a minimally invasive, continuously monitoring glucose sensing platform. This brief review thus demonstrates the tremendous potential for the application of SERS in biomedical research.

In the experiments described in this paper, citrate-reduced silver colloidal nanoparticles prepared according to a modified version of the Lee and Miesel method have been successfully used^{4,58} to obtain SERS spectra of the integrins $\alpha 5\beta 1$ and $\alpha V\beta 3$ that are present in vascular smooth muscle cells (VSMCs) and ECM. Of the many colloids available, the citrate-reduced silver colloids were the most attractive primarily due to the long-term stability of the colloids and the presence of a layer of citrate ion on the surface of the particle that controls protein adsorption and minimizes denaturation of the protein once adsorbed on the silver particle.⁵⁹ Typical citrate-reduced silver colloids are polydisperse, containing spherical, spheroidal, and other polygonal 3-D structured particles. The silver colloids used in our experiments were activated for aggregation prior to the addition of integrins with 1-M NaCl. The specific peaks that appear in the SERS spectra of the integrins adsorbed on the colloidal silver particles contain information about the structure of the part of the large integrin molecule that is in closest proximity to the charged colloidal surface [molecular weight (MW) of $\alpha 5\beta 1 = 265$ kDa, $\alpha V\beta 3 = 240$ kDa]. These include information on protein backbone structures such as amide vibrations, specific amino acid residues, as well certain bonds such as S-S (disulfide bridges) and C-H stretching vibrations among others that can help illustrate the secondary and tertiary structure of the adsorbed protein.

2 Materials and Methods

Citrate-reduced silver colloids were prepared according to a modified Lee and Miesel method.⁵⁸ All glassware were rigorously cleaned with nitric acid under a fume hood, and then rinsed with distilled water and scrubbed with soapy water followed by a final rinse with distilled water. Extinction spectra for the silver colloids were obtained using a Beckmann DU 640 spectrophotometer in the range of 300 to 800 nm using a standard 1-cm-path-length disposable polystyrene cuvette (VWR International Inc., West Chester, Pennsylvania). All SERS spectra were collected using a Renishaw System 1000 Raman Spectrometer coupled to a Leica DMLM microscope. The laser used was 514.5-nm Ar⁺ laser (Spectra Physics Model 263C) delivering approximately 4.50 mW power at the sample. SERS spectra were taken of purified human integrin $\alpha V\beta 3$ and $\alpha 5\beta 1$ (Cat. numbers CC1021 and CC1027, respectively, Chemicon International, Temecula, California) in 25-mM Tris-HCl, 150-mM NaCl, 1-mM MgCl₂, 0.1-mM

CaCl₂, 100-mM Octyl- β -D-Glucopyranoside buffer, pH = 7.4. The samples for the SERS tests were prepared by adding 5 μ l of 1-M NaCl to 50 μ l of the Ag colloid to activate it. After uniform mixing, 5 μ l of $\alpha V\beta 3$ integrin and $\alpha 5\beta 1$ integrin of various concentrations were added respectively to separate aliquots of activated Ag colloid mixtures. The final concentrations of $\alpha 5\beta 1$ integrin studied were 131, 66, and 33 nM and the $\alpha V\beta 3$ integrin concentrations studied were 122, 61, and 31 nM, respectively. SERS spectra of the samples were collected with the diffraction grating centered at 1200 cm⁻¹ with an integration time of 150 seconds for each scan. A third set of SERS spectra of Ag colloid, NaCl, and buffer was taken and served as a background. The final spectra presented in the following section are SERS spectra of the integrins with the background subtracted, on which a baseline correction routine was performed. The baseline correction routine used was a GRAMS/32 based routine (Galactic Industries Corporation, Salem, New Hampshire); which was a built-in feature of the WiRETM software (version 1.2) that controlled the Raman spectrometer.

3 Results and Discussion

The extinction spectra of the Ag colloids used in this study is shown in Fig. 1. The colloids have an extinction peak located at 425 nm with a full width at half maximum (FWHM) of 115 nm. This location of the extinction peak is due to the sum of the effects of light absorption and scattering, which in turn is dependent on the size and the dielectric constant of these particles and the surrounding media.⁶⁰ The broad FWHM of the Ag colloids used in these experiments points to the presence of a heterogeneous distribution of particle size and shapes in the colloidal mixture.

The raw (unprocessed) SERS spectra of 131-nM $\alpha 5\beta 1$ integrin, 122-nM $\alpha V\beta 3$, and colloid only (background spectra), offset for clarity, are shown in Fig. 2. As we can clearly see, both the integrin samples have several SERS peaks that are not present in the background. A careful examination of the spectra revealed subtle differences between the spectra of $\alpha 5\beta 1$ and $\alpha V\beta 3$. These differences are examined in detail later in the discussion.

The baseline-corrected and background-subtracted SERS spectra of 131-nM $\alpha 5\beta 1$ integrin is shown in Fig. 3 with the major SERS peak locations marked. A survey of existing literature tentatively reveals the bonds that are responsible for the appearance of the SERS peaks. The high correlation between the structural properties of the protein molecule and the location of its SERS peaks makes this technique a powerful tool for the detection of protein structure. All band assignments are tentative. The 1645-cm⁻¹ peak is the amide I band of the α -helix structure; and the 1306-cm⁻¹ peak lies in the region of the amide III band for the α -helix structure, thus suggesting that the $\alpha 5\beta 1$ integrin is adsorbed on the colloidal Ag particles in an α -helix region.^{32,33} Amides I and III are the peptide backbone modes. The amide I mode generally has a high contribution from the carbonyl stretching vibration. On the other hand, the amide III mode generally consists of the C-N-H in plane bending and C-N stretching modes.^{33,61} The peak located at 1569 cm⁻¹ originates from tryptophan, and the 1507-cm⁻¹ peak is from either phenylalanine or histidine.^{32,33} The peak located at 1359 cm⁻¹ can be attributed

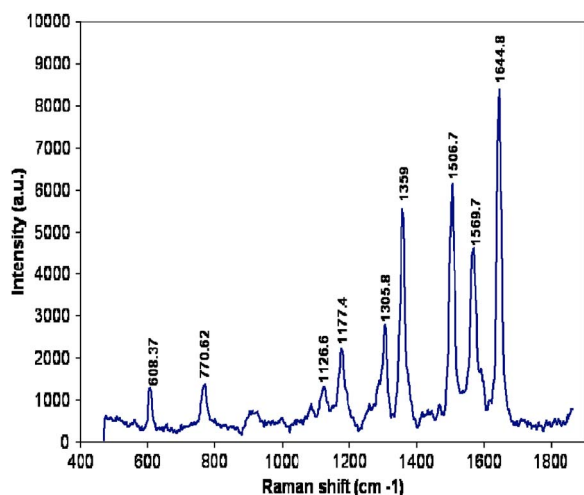


Fig. 3 Baseline-corrected and background-subtracted SERS spectra of 133-nM $\alpha 5\beta 1$ integrin.

to tryptophan vibration, which is sensitive to the environment of the indole rings.^{32,33,61} The fact that this band is so pronounced is indicative of the existence of a hydrophobic environment around the indole rings that is created by the aggregated Ag colloids.³² The peak located at 1177 cm^{-1} is the result of either tyrosine or phenylalanine, and the 1127- cm^{-1} peak can be assigned to the C–N bond stretching vibration.^{28,32,33,62} The 771- cm^{-1} peak can be attributed to either tryptophan or histidine, and the 608- cm^{-1} peak can be attributed to phenylalanine.^{32,33}

The SERS peaks of the $\alpha 5\beta 1$ integrin were sensitive to concentration. An examination of the average corrected SERS spectra of four consecutive scans of 133-, 66-, and 33-nM $\alpha 5\beta 1$ are shown, with an offset for visual clarity, in Fig. 4. Of the many SERS peaks available, the amide III peak at 1306 cm^{-1} , the phenylalanine or histidine peak at 1507 cm^{-1} ,

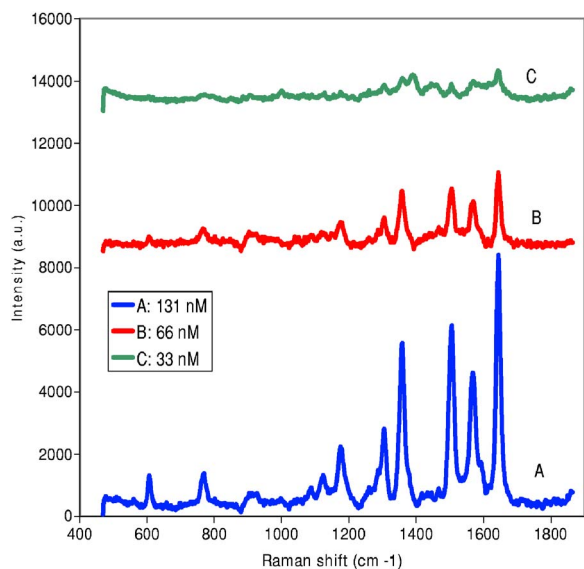


Fig. 4 Average of baseline-corrected and background-subtracted SERS spectra of four consecutive scans of 133-, 66-, and 33-nM $\alpha 5\beta 1$ integrin.

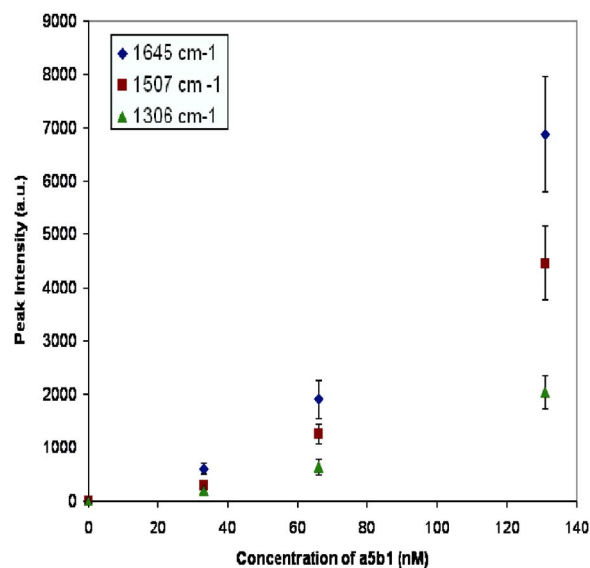


Fig. 5 Change in the height of (amide III) 1306 cm^{-1} , (Phe or His) 1507 cm^{-1} , and (amide I) 1645 cm^{-1} SERS peaks of $\alpha 5\beta 1$ integrin with varying concentrations.

and the amide I peak at 1645 cm^{-1} were used to analyze the concentration dependency of the SERS signal. Figure 5 shows the peak height of the 1306-, 1507-, and 1645- cm^{-1} peaks of the $\alpha 5\beta 1$ integrin at 0-, 33-, 66-, and 133-nM concentrations. The data points are the average of four scans at each concentration and the error bars represent the standard deviation of the four scans at each concentration. The graph shows an increase in the peak heights with concentration. Of the peaks analyzed, it is obvious that the amide I peak at 1645 cm^{-1} is most sensitive to concentration, followed by the 1507- cm^{-1} peak and then the amide III peak at 1306- cm^{-1} . Many SERS-based systems have a sigmoidal response of the SERS signal to analyte concentration, starting with an initial nonlinear response region at low analyte concentrations, followed by a linear region, and then subsequently another nonlinear region at high analyte concentrations.⁶³ For low concentrations of analyte, the SERS signal is generally nonlinear, as the colloidal system requires a minimum threshold number of active surface sites on the silver colloidal nanoparticles that must be utilized for the silver colloids to elicit a quantitative linear response with increasing concentration of analyte.⁶³ Additionally, in the low-analyte-concentration regime, the limit of detection is also compromised by the lower limit of the collection efficiency of the Raman spectrometer and CCD camera. This also plays a role in the apparent nonlinearity of the SERS signal at low analyte concentrations. This is then followed by the linear response regime. After complete saturation of the active sites on the silver colloidal nanoparticles, the system ceases to respond linearly to increased concentrations of the analyte. This leads to the second nonlinear region of the response curve at high concentrations of the analyte. The upper limit of the collection efficiency of the Raman spectrometer and CCD camera also plays a role in this nonlinearity.^{63–67} The nonlinearity of the data presented in this case indicates that the concentrations of $\alpha 5\beta 1$ integrins studied (as shown in Fig. 5) are at the lower end of the response curve and thus lie in the initial part of the sigmoidal response

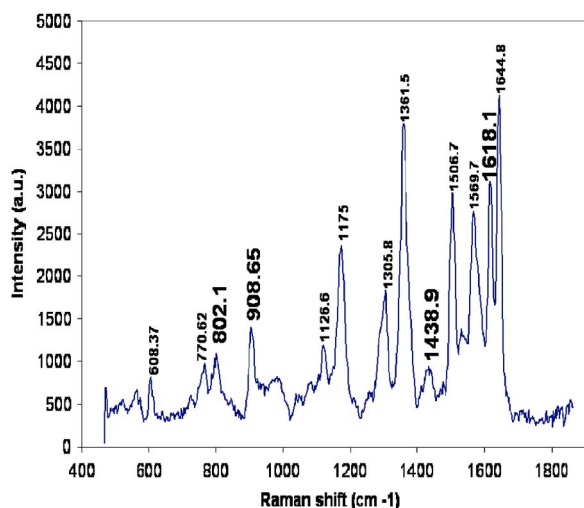


Fig. 6 Baseline-corrected and background-subtracted SERS spectra of 122-nM $\alpha V\beta 3$ integrin.

curve. The SERS signals below 30 nM were noisy and did not show a concentration-dependent characteristic (data not shown). Thus, the limit of detection for the $\alpha 5\beta 1$ integrin using this silver colloidal assay is approximately 30 nM.

The corrected SERS spectra of 122-nM $\alpha V\beta 3$ integrin is shown in Fig. 6 with the major SERS peak locations marked. Most of the SERS peaks of $\alpha V\beta 3$ are identical to those of $\alpha 5\beta 1$ except the four peaks marked in large bold numbers located at 1618, 1439, 908, and 802 cm^{-1} , respectively. The 1618- cm^{-1} peak originates from either of the aromatic amino acids tryptophan, tyrosine, or phenylalanine and the C α -C-N vibration at 908 cm^{-1} indicates the presence of α -helical structure in $\alpha V\beta 3$ in addition to its amide I and amide III peaks.^{32,33} The 1439- cm^{-1} peak results from the C-H₂ stretching vibrations, and the 802- cm^{-1} band also seems to originate from the protein backbone, as was observed previously.^{33,68} This shows that these two separate integrins adsorb with a different orientation on the surface of the Ag colloid and thus lends credibility to the idea that the two integrins are different in structure. Table 1 presents the tentative SERS peak assignments of both integrin molecules in a concise manner.

Figure 7 shows the height of the 1306-, 1507-, and 1645- cm^{-1} peaks for the $\alpha V\beta 3$ integrin at 0-, 61-, and 122-nM concentrations. The data points are the average of four scans at each concentration, and the error bars represent the standard deviation of the four scans at each concentration. Like the case of the $\alpha 5\beta 1$ integrin, the $\alpha V\beta 3$ integrins show a concentration dependence at 0, 61, and 122 nM. The SERS signals below 60 nM, however, were noisy and error prone and did not show a concentration-dependent characteristic (data not shown). The change in magnitude of the $\alpha V\beta 3$ integrin SERS signal with increasing concentration is lower when compared with the concentration response of the $\alpha 5\beta 1$ integrin. This might be the result of a lower affinity of the $\alpha V\beta 3$ integrin toward colloidal silver when compared to the $\alpha 5\beta 1$ integrin in the experimental conditions. The proposed lower affinity of the $\alpha V\beta 3$ integrin can be the result of subtle differences in its structure, which is revealed by its SERS

Table 1 Tentative SERS band assignments for $\alpha 5\beta 1$ and $\alpha V\beta 3$ integrins, where the bands in bold are unique only to $\alpha V\beta 3$

$\alpha 5\beta 1$ Band Frequency (cm^{-1})	$\alpha V\beta 3$ Band Frequency (cm^{-1})	Tentative Band Assignment
608	608	Phe
770	770	Trp or His
	802	Protein backbone
	908	C α -C-N
1126	1126	C-N bond
1175	1175	Tyr or Phe
1306	1306	Amide III (α -helix)
1361	1361	Trp
	1439	C-H ₂
1506	1506	Phe or His
1569	1569	Trp
	1618	Trp, Tyr, or Phe
1645	1645	Amide I (α -helix)

signature. This difference in structure between the two integrins can influence the orientation of the molecule in the silver binding site as well as strength of the bonds involved in adsorption of the integrins to the colloidal surface, and hence can govern the sensitivity of the SERS concentration response signal.

The preceding results demonstrate the ability of SERS to distinguish between the $\alpha 5\beta 1$ and $\alpha V\beta 3$ integrins and to detect them at varying concentrations to the nanomolar level. This first step shows the potential for using SERS in integrin detection by, for example, coating an atomic force microscope (AFM) tip with metal nanoparticles to map the distribution of cell surface integrins on VSMCs. Further, the long-term objective would be to use the SERS-AFM system to study the integrin interaction with the extracellular protein fibronectin. Currently AFM has been used to measure adhesion forces

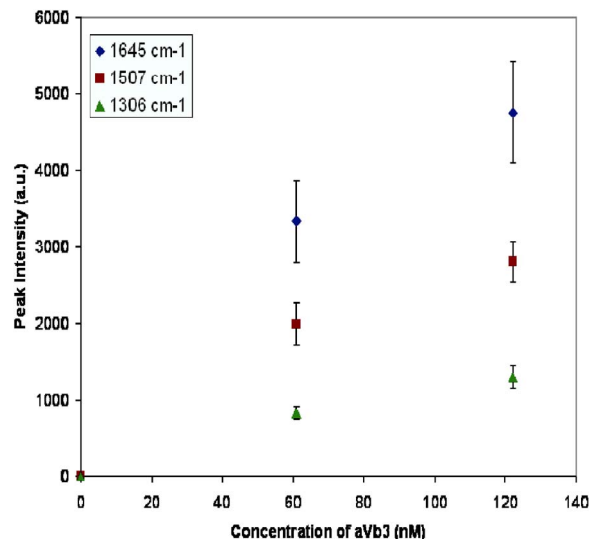


Fig. 7 Change in the height of (amide III) 1306- cm^{-1} , (Phe or His) 1507- cm^{-1} , and (amide I) 1645- cm^{-1} SERS peaks of $\alpha V\beta 3$ integrin with varying concentrations.

between integrins and fibronectin in VSMCs by coating the AFM tip with fibronectin, bringing the tip in contact with the cell surface, and then retracting the tip and analyzing the rupture forces between the two molecules⁴. Although this technique can detect the presence of cell-surface integrins, it still leaves some unanswered questions about structural changes occurring in the integrin molecule on binding and unbinding to fibronectin. This type of structural information might be crucial in understanding the role of integrins in the transmission of mechanical forces along the cell membrane that might be responsible for intracellular signaling⁴⁻⁷. SERS being sensitive to the structure of an analyte can potentially be used as a complementary technique to enhance the information obtained about the specifics of integrin-fibronectin interactions.

4 Conclusion

The ability to measure a SERS spectra of integrins was shown for the first time in this paper. It was shown that SERS is sensitive enough to not only detect but to distinguish the presence of various forms of integrin and is also responsive to their concentration levels. In the case of the $\alpha 5 \beta 1$ integrin, the SERS data showed a direct dependence on concentration. The limit of detection for the case of the $\alpha 5 \beta 1$ integrins was in the region of 30 nM. Using the same batch of silver colloidal nanoparticles, it was found that the SERS data in the case of the $\alpha V \beta 3$ integrins had a limit of detection in the region of 60 nM. This difference in the limit of detection of the two integrins can be attributed to a difference in their adsorption orientation and kinetics with the silver colloidal particles. It is apparent that the $\alpha 5 \beta 1$ integrin adsorbed more favorably to the silver colloidal particles. This difference in adsorption orientation can be attributed to differences in structure between the two protein molecules. It can be concluded from these experiments that SERS can indeed be used to detect the presence of various forms of integrins and thus provides optimism that this technique can potentially be exploited to map integrins on the surface of VSMCs and study their interactions with various ligands.

The next step in this study is combining the proposed SERS method with an AFM system. This will be done by coating the AFM tip with silver or gold followed by functionalizing the metal surface with fibronectin. It is thus expected that the SERS information obtained from the presence of integrins on the surface of VSMCs and the dynamic change in integrin structure on binding and unbinding with fibronectin, when coupled with the AFM force measurements might help to elucidate the mechanism of integrin-ligand interactions in vascular cells. This will hopefully promote new discoveries and insights about the nature of various cellular mechanotransduction processes.

Acknowledgments

This work was supported by the National Institutes of Health (NIH) Grants HL58960 and HL062863 and the Whitaker Foundation Special Opportunity Award.

References

1. A. F. Horwitz, "Integrins and health," *Sci. Am.* **68-75**, 68-75 (May 1997).
2. R. O. Hynes, "Integrins: bidirectional, allosteric signaling machines," *Cell* **110**, 673-687 (2002).
3. R. O. Hynes, "Integrins: versatility, modulation and signalling," *Cell* **69**(1), 11-25 (1992).
4. L. A. Martinez-Lemus, Z. Sun, A. Trache, J. P. Trzeciakowski, and G. A. Meininger, "Integrins and regulation of the microcirculation: from arterioles to molecular studies using atomic force microscopy," *Microcirculation (Philadelphia)* **12**, 1-14 (2005).
5. L. A. Martinez-Lemus, X. Wu, E. Wilson, M. A. Hill, G. E. Davis, M. J. Davis, and G. A. Meininger, "Integrins as unique receptors for vascular control," *J. Vasc. Res.* **40**, 211-233 (2003).
6. J. E. Mogford, G. E. Davis, S. H. Platts, and G. A. Meininger, "Vascular smooth muscle $\alpha v \beta 3$ integrin mediates arteriolar vasodilation in response to RGD peptides," *Circ. Res.* **79**, 821-826 (1996).
7. J. E. Mogford, G. E. Davis, and G. A. Meininger, "RGDN peptide interaction with endothelial $\alpha 5 \beta 1$ integrin causes sustained endothelin-dependent vasoconstriction of rat skeletal muscle arterioles," *J. Clin. Invest.* **100**, 1647-1653 (1997).
8. C. L. Stevenson and T. Vo-Dinh, "Signal expressions in Raman spectroscopy," *Modern Techniques in Raman Spectroscopy*, J. J. Laserna, Ed., pp. 1-39, John Wiley and Sons Publishers, West Sussex, England (1996).
9. A. Rupérez and J. J. Laserna, "Surface-enhanced Raman spectroscopy," in *Modern Techniques in Raman Spectroscopy*, J. J. Laserna, Ed., pp. 227-264, John Wiley and Sons Publishers, West Sussex, England (1996).
10. K. Kneipp, H. Kneipp, I. Itzkan, R. R. Dasari, and M. S. Feld, "Surface-enhanced Raman scattering and biophysics," *J. Phys.: Condens. Matter* **14**, R597-R624 (2002).
11. C. A. Murray, "Molecule-silver separation distance," in *Surface Enhanced Raman Scattering*, R. K. Chang and T. E. Furtak, Eds., pp. 203-221, Plenum Press, New York (1982).
12. M. Moskovits, "Surface-enhanced spectroscopy," *Rev. Mod. Phys.* **57**(3), 783-826 (1985).
13. F. J. Garcia-Vidal and J. B. Pendry, "Collective theory for surface enhanced Raman scattering," *Phys. Rev. Lett.* **77**(6), 1163-1166 (1996).
14. K. Kneipp, H. Kneipp, I. Itzkan, R. R. Dasari, and M. S. Feld, "Ultrasensitive chemical analysis by Raman spectroscopy," *Chem. Rev. (Washington, D.C.)* **99**, 2957-2975 (1999).
15. H. Xu, J. Aizpurua, M. Käll, and P. Apell, "Electromagnetic contribution to single-molecule sensitivity in surface-enhanced Raman scattering," *Phys. Rev. E* **62**(3), 4318-4324 (2000).
16. M. Käll, H. Xu, and P. Johansson, "Field enhancement and molecular response in surface-enhanced Raman scattering and fluorescence spectroscopy," *J. Raman Spectrosc.* **36**, 510-514 (2005).
17. M. Moskovits, "Surface-enhanced Raman spectroscopy: a brief retrospective," *J. Raman Spectrosc.* **36**, 485-496 (2005).
18. J. Jiang, K. Bosnick, M. Maillard, and L. Brus, "Single molecule Raman spectroscopy at the junctions of large Ag nanocrystals," *J. Phys. Chem. B* **107**, 9964-9972 (2003).
19. K. Kneipp, Y. Wang, H. Kneipp, L. V. Perelman, I. Itzkan, R. R. Dasari, and M. S. Feld, "Single molecule detection using surface enhanced Raman scattering (SERS)," *Phys. Rev. Lett.* **78**(9), 1667-1670 (1997).
20. S. Nie and S. R. Emory, "Probing single molecules and single nanoparticles by surface enhanced Raman scattering," *Science* **275**, 1102-1106 (1997).
21. W. E. Doering and S. Nie, "Single-molecule and single-nanoparticle SERS: examining the roles of surface active sites and chemical enhancement," *J. Phys. Chem. B* **106**, 311-317 (2002).
22. K. Kneipp, H. Kneipp, V. B. Kartha, R. Manoharan, G. Deinum, I. Itzkan, R. R. Dasari, and M. S. Feld, "Detection and identification of a single DNA base molecule using surface-enhanced Raman scattering (SERS)," *Phys. Rev. E* **57**(6), R6281-R6284 (1998).
23. J. T. Krug II, G. D. Wang, S. R. Emory, and S. Nie, "Efficient Raman enhancement of intermittent light emission observed in single gold nanocrystals," *J. Am. Chem. Soc.* **121**, 9208-9214 (1999).
24. A. Otto, "What is observed in single molecule SERS, and why?" *J. Raman Spectrosc.* **33**, 593-598 (2002).
25. Y. Maruyama and M. Futamata, "Elastic scattering and emission correlated with single-molecule SERS," *J. Raman Spectrosc.* **36**, 581-592 (2005).
26. A. Otto, A. Bruckbauer, and Y. X. Chen, "On the chloride activation in SERS and single molecule SERS," *J. Mol. Struct.* **661-662**, 501-

- 514 (2003).
27. G. D. Chumanov, R. G. Efremov, and I. R. Nabiev, "Surface-enhanced Raman spectroscopy of biomolecules," *J. Raman Spectrosc.* **21**, 43–48 (1990).
 28. S. K. Kim, M. S. Kim, and S. W. Suh, "Surface-enhanced Raman scattering (SERS) of aromatic amino acids and their glycyl dipeptides in silver sol," *J. Raman Spectrosc.* **18**, 171–175 (1987).
 29. I. R. Nabiev, V. A. Savchenko, and E. S. Efremov, "Surface-enhanced Raman spectra of aromatic amino acids and proteins by silver hydrosols," *J. Raman Spectrosc.* **14**(6), 375–379 (1983).
 30. X. Dou, Y. M. Jung, H. Yamamoto, S. Doi, and Y. Ozaki, "Near-infrared excited surface-enhanced Raman scattering of biological molecules on gold colloid I: effects of pH of the solutions of amino acids and their polymerization," *Appl. Spectrosc.* **53**(2), 133–138 (1999).
 31. X. Dou, Y. M. Jung, Z.-Q. Cao, and Y. Ozaki, "Surface-enhanced Raman scattering of biological molecules on metal colloid II: effects of aggregation of gold colloid and comparison of effects of pH of glycine solutions between gold and silver colloids," *Appl. Spectrosc.* **53**(11), 1440–1447 (1999).
 32. H. Deng, Q. He, Z. Xu, X. Wang, and R. Sheng, "The study of turnip mosaic virus coat protein by surface enhanced Raman spectroscopy," *Spectrochim. Acta, Part A* **49**(12), 1709–1714 (1993).
 33. J. Hu, R. S. Sheng, Z. S. Xu, and Y. Zeng, "Surface enhanced Raman spectroscopy of lysozyme," *Spectrochim. Acta, Part A* **51**(6), 1087–1096 (1995).
 34. S. C. Pízarzu, S. Cavalu, N. Leopold, R. Petry, and W. Keifer, "Raman and surface-enhanced Raman spectroscopy of tempyo spin labeled ovalbumin," *J. Mol. Struct.* **565–566**, 225–229 (2001).
 35. P. Miškovský, D. Jancura, S. S. Cortés, E. Kočíšová, and L. Chinsky, "Antiretrovirally active drug hypericin binds the IIA subdomain of human serum albumin: resonance Raman and surface-enhanced Raman spectroscopy study," *J. Am. Chem. Soc.* **120**, 6374–6279 (1998).
 36. P. Miskovsky, J. Hritz, S. S. Cortes, G. Fabriciova, J. Ulicny, and L. Chinsky, "Interaction of hypericin with serum albumins: surface enhanced Raman spectroscopy and molecular modeling study," *Photochem. Photobiol.* **74**(2), 172–183 (2001).
 37. N. H. Jang, "The coordination chemistry of DNA nucleosides on gold nanoparticles as a probe by SERS," *Bull. Korean Chem. Soc.* **23**(12), 1790–1800 (2002).
 38. K. Kneipp and J. Flemming, "Surface enhanced Raman scattering (SERS) of nucleic acids adsorbed on colloidal silver particles," *J. Mol. Struct.* **145**, 173–179 (1986).
 39. K. Kneipp, W. Pohle, and H. Fabian, "Surface enhanced Raman spectroscopy of nucleic acids and related compounds adsorbed on colloidal silver particles," *J. Mol. Struct.* **244**, 183–192 (1991).
 40. J. Thorton and R. K. Force, "Surface-enhanced Raman spectroscopy of nucleic acid compounds and their mixtures," *Appl. Spectrosc.* **45**(9), 1522–1526 (1991).
 41. S. K. Kim, T. H. Joo, S. W. Suh, and M. S. Kim, "Surface-enhanced Raman scattering (SERS) of nucleic acid components in silver sol: adenine series," *J. Raman Spectrosc.* **17**, 381–386 (1986).
 42. L. A. Gearheart, H. J. Ploehn, and C. J. Murphy, "Oligonucleotide adsorption to gold nanoparticles: a surface-enhanced Raman spectroscopy study of intrinsically bent DNA," *J. Phys. Chem. B* **105**, 12609–12615 (2001).
 43. K. Kneipp, A. S. Haka, H. Kneipp, K. Badizadegan, N. Yoshizawa, C. Boone, K. E. Shafer-Peltier, J. T. Motz, R. R. Dasari, and M. S. Feld, "Surface enhanced Raman spectroscopy in single living cells using gold nanoparticles," *Appl. Spectrosc.* **56**(2), 150–154 (2002).
 44. W. R. Premasiri, D. T. Moir, M. S. Klemper, N. Krieger, G. Jones II, and L. D. Ziegler, "Characterization of the surface enhanced Raman scattering (SERS) of bacteria," *J. Phys. Chem. B* **109**, 312–320 (2005).
 45. L. R. Allain and T. Vo-Dinh, "Surface-enhanced Raman scattering detection of the breast cancer susceptibility gene BRCA1 using silver-coated microarray platform," *Anal. Chim. Acta* **469**, 149–154 (2002).
 46. T. Vo-Dinh, L. R. Allain, and D. L. Stokes, "Cancer gene detection using surface-enhanced Raman scattering (SERS)," *J. Raman Spectrosc.* **33**, 511–516 (2002).
 47. T. Vo-Dinh, D. L. Stokes, G. D. Griffin, M. Volkan, U. J. Kim, and M. I. Simon, "Surface-enhanced Raman scattering (SERS) method and instrumentation for genomics and biomedical analysis," *J. Raman Spectrosc.* **30**, 785–793 (1999).
 48. X. Dou, T. Takama, Y. Yamaguchi, and H. Yamamoto, "Enzyme immunoassay utilizing surface-enhanced Raman scattering of the enzyme reaction product," *Anal. Chem.* **69**, 1492–1495 (1997).
 49. S. R. Hawi, S. Rochanakij, F. Adar, W. B. Campbell, and K. Nithipatikom, "Detection of membrane-bound enzymes in cells using immunoassay and Raman microspectroscopy," *Anal. Biochem.* **259**, 212–217 (1998).
 50. Y. W. C. Cao, R. C. Jin, and C. A. Mirkin, "Nanoparticles with Raman spectroscopic fingerprints for DNA and RNA detection," *Science* **297**, 1536–1540 (2002).
 51. Y. C. Cao, R. C. Jin, J. M. Nam, C. S. Thaxton, and C. A. Mirkin, "Raman dye-labeled nanoparticle probes for proteins," *J. Am. Chem. Soc.* **125**, 14676–14677 (2003).
 52. D. A. Stuart, A. J. Haes, A. D. McFarland, S. Nie, and R. P. Van Duyne, "Refractive index sensitive, plasmon resonant scattering, and surface enhanced Raman scattering nanoparticles and arrays as biological sensing platforms," *Proc. SPIE* **5327**, 60–73 (2004).
 53. S. P. Mulvaney, M. D. Musick, C. D. Keating, and M. J. Natan, "Glass coated, analyte tagged nanoparticles: a new tagging based on detection with surface-enhanced Raman scattering," *Langmuir* **19**, 4784–4790 (2003).
 54. X. Zhang, M. A. Young, O. Lyandres, and R. P. Van Duyne, "Rapid detection of an anthrax biomarker by surface enhanced Raman spectroscopy," *J. Am. Chem. Soc.* **127**, 4484–4489 (2005).
 55. C. L. Haynes, C. R. Yonzon, X. Zhang, and R. P. Van Duyne, "Surface-enhanced Raman sensors: early history and the development of sensors for quantitative biowarfare agent and glucose detection," *J. Raman Spectrosc.* **36**, 471–484 (2005).
 56. K. E. Shafer-Peltier, C. L. Haynes, M. R. Glucksberg, and R. P. Van Duyne, "Toward a glucose biosensor based on surface enhanced Raman scattering," *J. Am. Chem. Soc.* **125**, 588–593 (2003).
 57. A. Stuart, C. R. Yonzon, X. Zhang, O. Lyandres, N. C. Shah, M. R. Glucksberg, J. T. Walsh, and R. P. Van Duyne, "Glucose sensing using near-infrared surface enhanced Raman spectroscopy: gold surfaces, 10-day stability, and improved accuracy," *Anal. Chem.* **77**, 4013–4019 (2005).
 58. P. C. Lee and D. Miesel, "Adsorption and surface-enhanced Raman of dyes on silver and gold sols," *J. Phys. Chem.* **86**, 3391–3395 (1982).
 59. C. H. Munro, W. E. Smith, M. Garner, J. Clarkson, and P. C. White, "Characterization of the surface of a citrate-reduced colloid optimized for use as a substrate for surface-enhanced resonance Raman scattering," *Langmuir* **11**, 3712–3720 (1995).
 60. G. Mie, "Beitrag zur optik trüber medien, speziell kolloidaler metallösungen," *Ann. Phys.* **25**, 377–445 (1908).
 61. L. Stryer, *Biochemistry*, 4th ed., W. H. Freeman and Company, New York (1995).
 62. S. Stewart and P. M. Fredericks, "Surface enhanced Raman spectroscopy of peptides and proteins adsorbed on an electrochemically prepared silver surface," *Spectrochim. Acta, Part A* **55**, 1615–1640 (1999).
 63. P. D. O'Neal, "The application of surface-enhanced Raman spectroscopy for the detection of excitatory amino acids," Biomedical Engineering Thesis, Texas A&M University (1999).
 64. D. A. Weitz, S. Garoff, J. I. Gersten, and A. Nitzan, "The enhancement of Raman scattering, resonance Raman scattering, and fluorescence from adsorbed on a rough silver surface," *J. Chem. Phys.* **78**(9), 5324–5338 (1983).
 65. A. Feofanov, A. Ianoul, S. Gromov, O. Fedorova, M. Alifimov, and I. Nabiev, "Complexation of photochromic Crown ether styryl dyes with Mg²⁺ as probed by surface enhanced Raman spectroscopy," *J. Phys. Chem. B* **101**, 4077–4084 (1997).
 66. S. E. J. Bell and N. M. S. Sirimuthu, "Rapid, quantitative analysis of ppm/ppb nicotine using surface enhanced Raman scattering from polymer-encapsulated Ag nanoparticles (gel-colls)," *Analyst (Cambridge, U.K.)* **129**, 1032–1036 (2004).
 67. A. G. Brolo, D. E. Irish, G. Szymanski, and J. Lipkowski, "Relationship between SERS intensity and both surface coverage and morphology for pyrazine adsorbed on a polycrystalline gold electrode," *Langmuir* **14**, 517–527 (1998).
 68. Z. Q. Wen, S. A. Overman, P. Bondre, and G. J. Thomas, Jr., "Structure and organization of bacteriophage Pf3 probed by Raman and ultraviolet resonance Raman spectroscopy," *Biochemistry* **40**, 449–458 (2001).